EPJ Web of Conferences **182**, 03013 (2018) https://doi.org/10.1051/epjconf/201818203013
ICNFP 2017

Antiproton-nucleus annihilation cross section at low energy

H. Aghai–Khozani[1], A. Bianconi[2,3], M. Corradini[2,3], R. Hayano[4], M. Hori[1,4], M. Leali[2,3], E. Lodi–Rizzini[2], V. Mascagna[2,3,a], Y. Murakami[4], M. Prest[5,6], E. Vallazza[8], L. Venturelli[2,3], and H. Yamada[4]

[1] *Max-Planck-Institut für Quantenoptik, D-85748 Garching, Germany*
[2] *Dipartimento di Ingegneria dell'Informazione, Università degli Studi di Brescia, I-25123 Brescia, Italy*
[3] *Istituto Nazionale di Fisica Nucleare - Pavia, I-27100 Pavia, Italy*
[4] *Department of Physics, University of Tokyo, Bunkyo-ku, Tokyo 113-0033, Japan*
[5] *Dipartimento di Scienza e Alta Tecnologia, Università degli Studi dell'Insubria, I-22100 Como, Italy*
[6] *Istituto Nazionale di Fisica Nucleare - Milano Bicocca, I-20126 Milano, Italy*
[7] *Istituto Nazionale di Fisica Nucleare - Trieste, I-34127 Trieste, Italy*

Abstract. The antinucleon-nuclei annihilation cross sections at low energies were systematically measured at CERN in the 80's and 90's with the LEAR facility and later with the Antiproton Decelerator. Unfortunately only few data exist for very low energy antiprotons (p<500 MeV/c) on medium and heavy nuclei. A deeper knowledge is required by fundamental physics and can have consequence also in cosmology and medical physics. In order to fill the gap, the ASACUSA Collaboration has very recently measured the annihilation cross section of 100 MeV/c antiprotons on carbon. In the present work the experimental result is presented together with a comparison both with the antineutron data on the same target at the same energies and with the other existing antiproton data at higher energies.

1 Introduction

The knowledge of the features of the nuclear interaction of low-energy antinucleons with matter is of interest both in nuclear physics and in fundamental cosmology. In particular the study of the annihilation process can be useful both to determine the parameters of the strong interaction in the quark and optical potential models, and to quantify signals of the presence of antimatter in the Universe to study the matter-antimatter asymmetry.

Systematic measurements were performed at LEAR in the 80's and 90's with antiprotons ($\bar{p}$) [1–13] and antineutrons ($\bar{n}$) [14–19] at energies below 50 MeV and also with antiprotonic atoms (see [20]). Recently the ASACUSA Collaboration has measured the annihilation cross section (σ_{ann}) of antiprotons at the Antiproton Decelerator (AD) of CERN [21, 22] at 5.3 MeV on medium and medium-heavy targets (Ni, Sn, Pt)[23].

The existing antinucleon–nucleus annihilation data at small (positive) energies and for $A > 4$ (A is the mass number) present unexplained features. In the region 300-400 MeV/c the $\bar{p}$ and $\bar{n}$ σ_{ann} values

[a] Now at Dipartimento di Scienza e Alta Tecnologia, Università degli Studi dell'Insubria, I-22100 Como, Italy and Istituto Nazionale di Fisica Nucleare - Milano Bicocca, I-20126 Milano, Italy

are similar [19], as expected, but they are higher than the predictions from optical models which well describe both the values at higher energies and the antiprotonic atoms data [24]. At lower energies, where the energy dependence of the $\bar{p}$ σ_{ann} should be different from $\bar{n}$ σ_{ann} due to the focusing effect on the charged projectile from the Coulomb attraction of the nucleus, the $\bar{n}$ data on several nuclei (C, Al, Cu, Ag, Sn, Pb) at momenta below 180 MeV/c [19] show an anomalous behavior. Their trends follow a $1/p^2$ dependence (p is momentum), which is typical of charged projectiles (like the antiproton), instead of $1/p$ expected for neutral particles.

More information is needed to clarify this puzzle. For this purpose it has been recently claimed [24] that a comparison of $\bar{p}$ and $\bar{n}$ σ_{ann}s on the same targets at the same energies can be useful.

In this work we present the measurement result of $\bar{p}$–C σ_{ann} at 5.3 MeV which can be immediately compared with the existing $\bar{n}$-C result in the same energy region.

2 Experimental method and apparatus

The measurement has been performed at AD [25–29] which is presently the only existing source of slow antiprotons. The $\bar{p}$s delivered by AD have a momentum p = 100 MeV/c (corresponding to an energy of 5.3 MeV) with a spread of $\Delta p/p = 0.01\%$ and an emittance of (2-3)π mm mrad. Each AD bunch contains $2-4\times10^7$ antiprotons with a time length of $\sim$ 200 ns and a repetition rate of 0.01 Hz.

Since the pulsed nature of the AD beam is not suitable for performing measurements of rare events, like in-flight annihilations, we developed an original experimental technique based on the experience we gained in previous experiments both at 5.3 MeV [23, 30] and at 130 keV [31–33].

The measurement technique consists in counting the in-flight antiproton annihilations N_{target} on a solid carbon target in comparison with the annihilations N_{ring} of the antiprotons diffused by the target on a ring (named "2nd ring") placed downstream, see [34] for more details.

The apparatus has been designed with a particular attention to separate in time the $\bar{p}$ annihilations on the target and on the 2nd ring from those on the rest of the apparatus.

Fig. 1 shows a sketch of the apparatus. It consists of: 1) a vacuum chamber made by two cylinders (120 cm in diameter and 130 cm in length the first one, 60 cm in diameter and 130 cm in length the second one) containing the target and the 2nd ring; 2) a scintillating bars detector (named "D1") which surrounds the vacuum chamber to count the annihilations on the target and on the 2nd ring; 3) two Čherenkov counters to measure the time duration and the intensity of the $\bar{p}$ beam; 4) two GEM detectors to focus the $\bar{p}$ on the target.

The antiprotons from AD first enter into the first cylinder (directly connected to the AD beam line) and then hit the carbon target placed 45 cm downstream the entrance of this cylinder. Only a small fraction will annihilate in-flight on the target while most of the antiprotons annihilate at the end of the apparatus.

D1 [35] counts the annihilations on the target and, when inserted, on the 2nd ring by recording the signals of the charged particles (mostly pions) emitted from the annihilations. It consists of 3 modules placed around the first cylinder (sideways and below) close to the target position and of 4 modules which are positioned more externally. The bars numbers of the modules range from 24 to 62. Each bar has a section of 1.5×1.9 cm^2 and a length of 96 cm. Their light is read by Hamamatsu 64 channels PMTs whose analog signals are acquired by dedicated front–end boards. Although D1 is arranged as a hodoscope and can measure and count the annihilation vertices by reconstructing the tracks of the emitted charged pions, in order to increase the statistics we prefer to count the fired channels of D1, whose number is proportional to the annihilations events.

The targets are thin disks (nominal thickness of 700 nm and 1000 nm) of diamond-like carbon made by Micromatter [36]. The uncertainty of the thickness (2-3%) is unimportant for the σ_{ann}

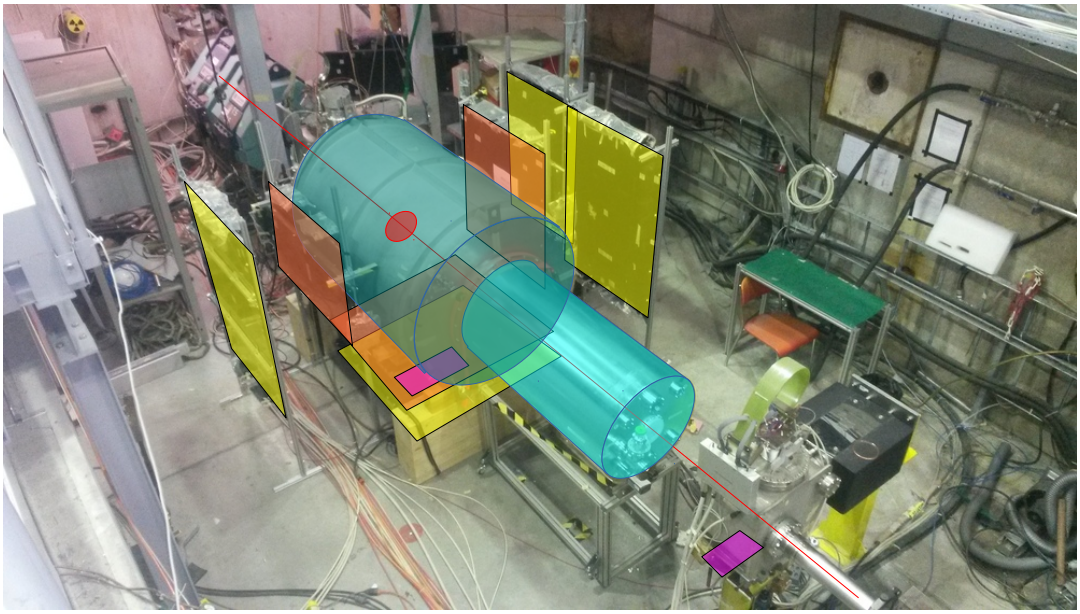

Figure 1. Picture of the apparatus: the vacuum chamber (in light blue); the target (in red); the inner (in orange) and the outer modules (in yellow) of the scintillator bars detector; the two Čherenkov detectors (in violet).

measurement, see below. The targets are mounted on rings with an internal diameter = 10 cm and an external diameter = 13 cm. The quite large radius of the targets strongly reduces the background of the antiprotons annihilating on the target frame.

The 2nd ring (inner diameter = 6 cm, outer diameter = 11 cm) is placed 15 cm downstream the target. It intercepts the antiprotons scattered by the target in a selected solid angle ($\Delta\Omega$).

The measurement of σ_{ann} is obtained by

$$\sigma_{ann} = \frac{N_{target}}{N_{ring}} \sigma_{scatt} \tag{1}$$

where N_{target} is the number of the annihilations in the target, N_{ring} is the number of the antiprotons diffused from the target on the 2nd ring (i.e. in $\Delta\Omega$) and σ_{scatt} is the scattering cross section in $\Delta\Omega$.

The finite time resolution of D1 (few ns as standard deviation) does not allow to distinguish an annihilation on the target from that on the 2nd ring, since the antiproton time-of-flight from the target to the 2nd frame is only ~5 ns. To determine N_{target} and N_{ring} we perform separate data acquisitions with only the target ("only-target run") and with target and 2nd ring together ("2nd-ring run"), as better described below.

The background of the annihilations on the target support is measured in specific runs where the target is replaced by its frame ("empty-target run").

All the counts of the different runs are normalized to the signal of the annihilations at the end of the apparatus, as detected by a Čherenkov detector (BIM) [37] (see Fig. 1), whose value is a measure of the incident $\bar{p}$ beam intensity.

Since both N_{target} and N_{ring} are actually measured by the same detector D1, the detection efficiency, which should appear both at the numerator and to the denominator of Equation 1, does not affect the σ_{ann} measure. A similar argument is valid for the target thickness, too.

We use the so-called "Multiple Extraction" mode of AD: each $\bar{p}$ bunch is divided in 6 pulses, each with about 5×10^6 particles and with a reduced time length. By tuning the AD kicker time we further reduce the duration of the first bunch to ~50 ns with a rise time of ~15 ns. This allows to distinguish the target signal from the background of the $\bar{p}$ annihilations occurring on the rest of the apparatus.

3 Results

The time distributions of the hits recorded by the inner modules of D1 are plotted in Fig. 2 for the only-target runs (black line), the 2nd-ring runs (red line) and the empty-target runs (blue line).

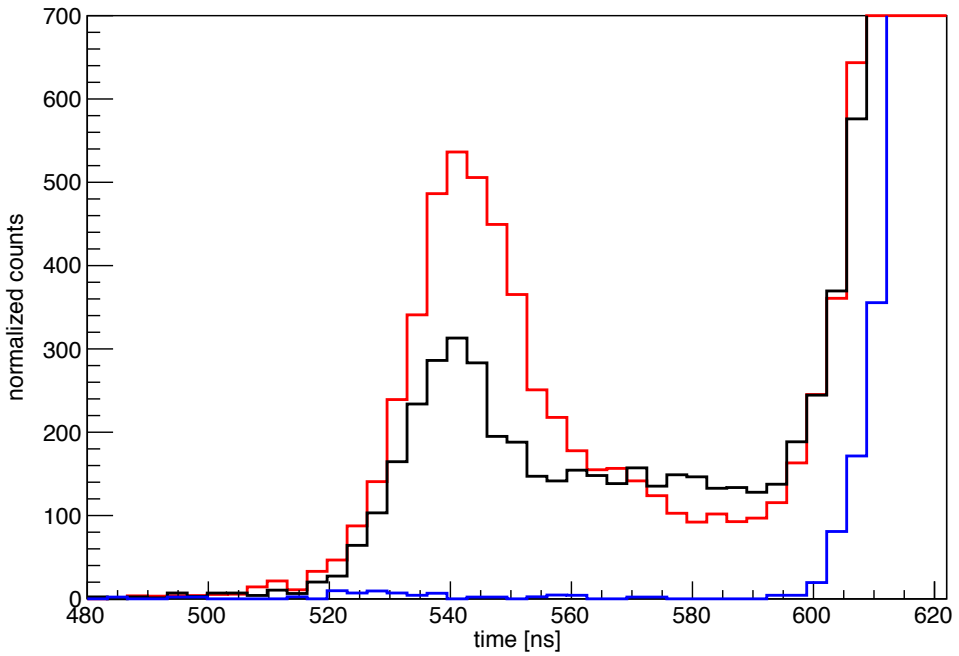

Figure 2. Time distributions recorded by the inner modules of D1: the black line for the only-target runs; the red line for 2nd-ring runs; the blue line for the empty-target runs.

A peak at around 535 ns clearly appears in the black and red distributions in correspondence of the $\bar{p}$ annihilations on the target and on the 2nd ring.

The annihilations after the peak come from the antiprotons scattered by the target on the vacuum chamber walls while the saturated signal starting at ~600 ns comes from the annihilations on the final walls of the 2 cylinders.

The blue histogram shows that the contribution of the background events from the target frame is small compared with the other distributions.

It is expected that the events on the lateral walls of the vacuum chamber start ∼20 ns after the first annihilations on the target since the 5.3 MeV $\bar{p}$ velocity is ∼3 cm/ns and the first cylinder has a 60 cm radius. This means that the second half of the peak at around 535 ns can be contaminated by this background. For this reason we select suitable fiducial time intervals in the first part of the peak to count the annihilations on the target, N_{target}, and on the 2nd ring, N_{ring}. In ΔT = 520–535 ns we count annihilations on the target by using the data of the only-target runs (the result is called M_{ann}), whereas in $\Delta T'$=525-540 ns we evaluate annihilations on the second ring by subtracting M_{ann} from the counts of the 2nd-ring runs (the result is called M'_{ring}). The shift of 5 ns between $\Delta T'$ and ΔT corresponds to the $\bar{p}$ time-of-flight from the target to the 2nd ring.

Before the described procedure, we multiply the counts of every run by a variable factor which corrects the saturation effect of D1 occuring when more charged particles simultaneously hit a bar (detection dead time of the order of 100 ns). This factor has been evaluated with Monte Carlo simulations and in the worst case its value is 15%.

The M_{ann} and M'_{ring} values can be used in Equation 1 to measure σ_{ann} since $M_{ann}/M'_{ring} \approx N_{target}/N_{ring}$.

The M_{ann}/M'_{ring} value results to be 1.01 ± 0.09 (the last value is the statistical error).

The σ_{scatt} value in Equation 1 depends on the Coulomb elastic scattering and on the experiment geometry. It is determined by Monte Carlo simulations based on the GEANT package where we use the Molière-Bethe formulation to describe the multiple scattering.

In the end the $\bar{p}$–C annihilation cross section at 5.3 MeV results to be σ_{ann} = (1.73 ± 0.25) barn. The error is the quadratic sum of the statistical (9%) and the systematic (11%) errors.

The systematic error comes from different contributions. The time resolution of D1 is estimated to give a 4% error. The correction of the saturation effect of D1 produces a 5% error. The σ_{scatt} value is affected by 1.5% error due to the ±1 mm uncertainty of the distance from the target to the 2nd ring and by 6% error from the uncertainty on the radial extension of the $\bar{p}$ beam. In addition we assume a 4% error due to the uncertainty of the Monte Carlo simulations based on the Molière-Bethe formulation which resulted to be valid for protons in similar conditions [38] but never tested for antiprotons. The uncertainty on the BIM signals yields 5% error in the normalization of the events.

4 Conclusions

The present result is shown in Fig. 3 together with the existing measurements on the same target with both antiprotons [39] and antineutrons [19], and with the predictions by the optical potential models of Ref. [24], Ref. [40] and Ref. [41].

It looks that there is no difference in the energy dependence for the two antinucleons on the carbon target, in contradiction with the expectations of higher antiproton values compared to the antineutron one when the focussing effect of the nucleus on a slow charged particle is considered.

In addition the considered theoretical models, based on different approaches, considerably underestimate both the antiproton and antineutron σ_{ann} values.

The $\bar{N}$−nucleus σ_{ann} calculated in Ref. [24] are determined with an optical potential tuned on the antiprotonic data and on the elastic scattering values up to 600 MeV/c.

In Ref. [40] the calculations are performed with an extended Glauber model evaluated by considering the transmission through a nuclear potential and the $\bar{p}$p Coulomb interaction.

The authors of Ref. [40] use also a phenomenological optical model with parameters tuned to reproduce the $\bar{N}$−nucleus σ_{ann} [41].

With the obvious exception of the last case, the disagreement between theoretical predictions and experimental data is evident. No clear explanation is available to us to explain that discrepancy.

The present measurement can be extended to medium-heavy targets by means of the same apparatus with the same technique. Also the antiproton nuclear elastic cross section on different nuclei can be measured by scanning the distance of the 2nd ring from the target in order to explore large angle regions (> 30°), where the nuclear effects can appear and no data exist at these energies.

In few years when the ELENA facility will be ready, the $\bar{p}$ σ_{ann} can be measured even at 100 keV, as already demonstrated by ASACUSA at AD [31–33] .

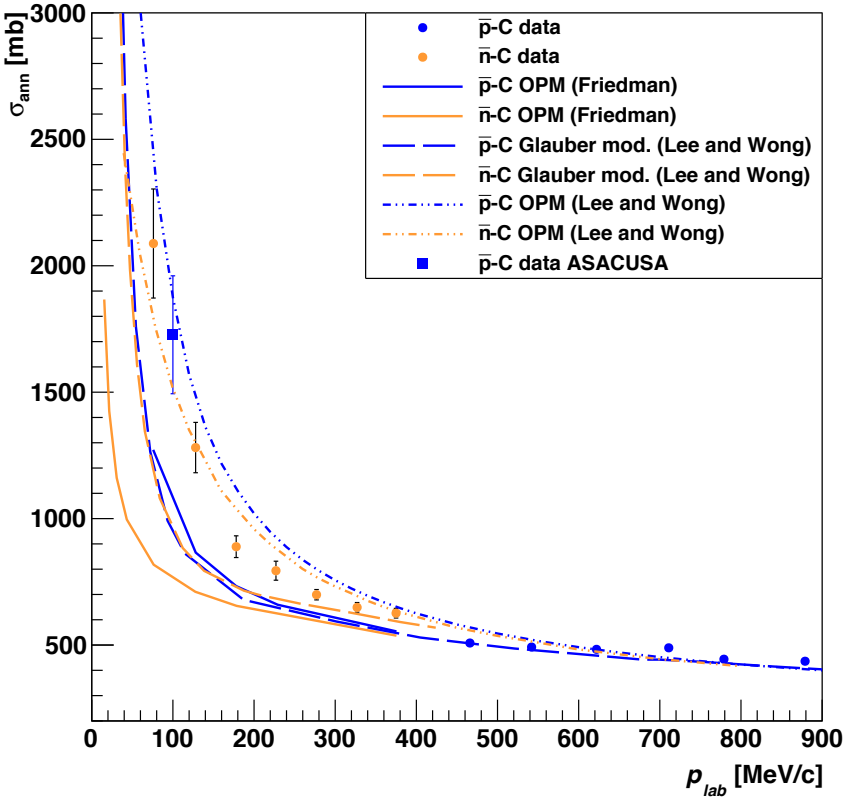

Figure 3. σ_{ann} at low energies on carbon for $\bar{p}$ (in blue) and for $\bar{n}$ (in orange). The present measurement is the value at p_{lab} = 100 MeV/c while the $\bar{p}$ data for p_{lab} > 400 MeV/c come from Ref. [39]. The $\bar{n}$ measurements are from Ref. [19]. The lines are theoretical calculations, see text for details.

5 Acknowledgments

We thank the CERN AD staff and all the other members of the ASACUSA Collaboration for the help and support. This work was supported by Istituto Nazionale di Fisica Nucleare (INFN), Università degli Studi di Brescia, Max-Planck-Gesellschaft and the European Research Council (ERC-Stg).

References

[1] R. Bizzarri et al., Nuovo Cimento A, 22 (1974) p.225
[2] T.E. Kalogeropoulos, G.S. Tzanakos, Phys. Rev. D, 22 (1980) p.2585
[3] F. Balestra et al., Phys. Lett. B, 149 (1984) p.69
[4] F. Balestra et al., Phys. Lett. B, 165 (1985) p.265
[5] F. Balestra et al., Nucl. Phys. A, 452 (1986) p.573
[6] F. Balestra et al., Phys. Lett. B, 230 (1989) p.36
[7] W. Brückner et al., Z. Phys. A, 335 (1990) p.217
[8] A. Bertin et al. (OBELIX Collaboration), Phys. Lett. B, 369 (1996) p.77
[9] A. Benedettini et al. (OBELIX Collaboration), Nucl. Phys. B, (Proc. Suppl.) 56A (1997) p.58
[10] A. Zenoni et al. (OBELIX Collaboration), Phys. Lett. B, 461 (1999) p.405
[11] A. Zenoni et al. (OBELIX Collaboration), Phys. Lett. B, 461 (1999) p.413
[12] A. Bianconi et al., Phys. Lett. B, 481 (2000) p.194
[13] A. Bianconi et al., Phys. Lett. B, 492 (2000) p.254
[14] B. Gunderson et al., Phys. Rev. D, 23 (1981) p.587
[15] M. Agnello et al., Europhys. Lett., 7 (1988) p.13
[16] C. Barbina et al., Nucl. Phys. A, 612 (1997) p.346
[17] V.G. Ableev et al., Nuovo Cimento A, 107 (1994) 943
[18] F. Iazzi et al. (OBELIX Collaboration), Phys. Lett. B, 475 (2000) p.378
[19] M. Astrua et al., Nucl. Phys. A, 697 (2002) pp.209—224
[20] A. Trzcinska et al., Nucl.Phys. A, 692 (2001) pp.176–181
[21] S. Maury, Hyperfine Interact., 43 (1997) p.109
[22] P. Belochitskii, T. Eriksson, S. Maury, Nucl. Instrum. Methods Phys. Res. A 214 (2004) p.176.
[23] A. Bianconi et al., Phys. Lett. B, 704 (2011) p.461.
[24] E.Friedman, Nucl. Phys. A, 925 (2014) pp.141—149
[25] G. Gabrielse, et al. Phys. Rev. Lett. 108 (2012) p.113002
[26] N. Kuroda, et al., Nature Commun. 5 (2014) p.3089
[27] M. Hori, et al., Science 354 (2016) pp.610–614
[28] M. Ahmadi, et al., Nature 541 (2017) pp.506–510
[29] M. Hori and J. Waltz, Prog. Part. Nucl. Phys. 72 (2013) 206
[30] M. Corradini et al., Nucl. Instr. Methods A 711 (2013) 12
[31] H. Aghai-Khozani et al., European Physical Journal Plus 127 (2012) 55
[32] K. Todoroki et al., Nucl. Instr. Methods A 835 (2016) 110
[33] H. Aghai-Khozani et al., to be submitted
[34] H. Aghai-Khozani et al., these proceedings, (2017)
[35] M. Corradini et al., Hyp. Int. 233 (2015) 53
[36] http://www.micromatter.com/dlc.php
[37] M. Hori et al., Nucl. Instrum. Methods A 496 (2003) 102
[38] H. Bichsel, Phys. Rev. 112 (1958) 182.
[39] K.Nakamura et al., Phys. Rev. Lett. 52 731 (1984)
[40] T. G. Lee and C. Y. Wong, Phys. Rev. C 93 (2016) 014616
[41] T.G. Lee, C.Y. Wong, private communication